p-process in SNIa and Galactic chemical evolution: what has been done and what has to be done

Travaglio C. (INAF-Astrophysical Observatory Turin,Italy)

COLLABORATORS:

Gallino R.,

Röpke F., Seitenzahl I., Hillebrandt W.,

Rauscher T., Reifarth R., Göbel K.,

Dauphas N.

COMPUTER RESOURCES: B2FH Ricerca per l'Astrofisica Nucleare — GOETHE UNIVERSITÄT FRANKFURT AM MAIN

35 *p-nuts*
Arnould (2003)

Routes to p-nuts

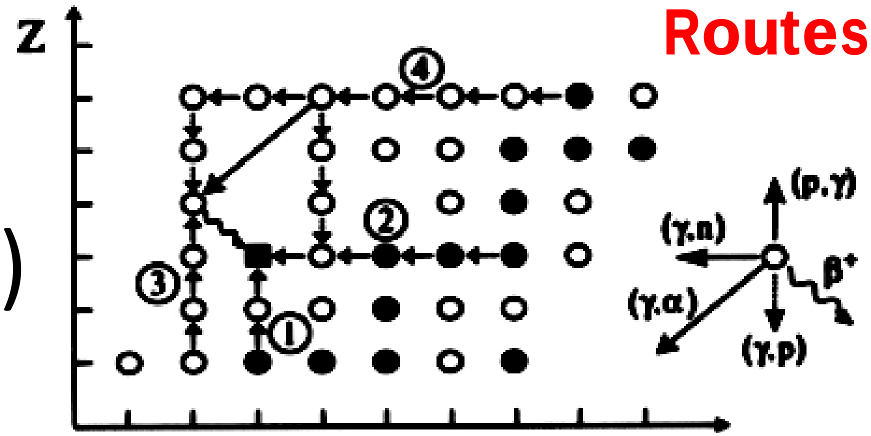

In the Solar System

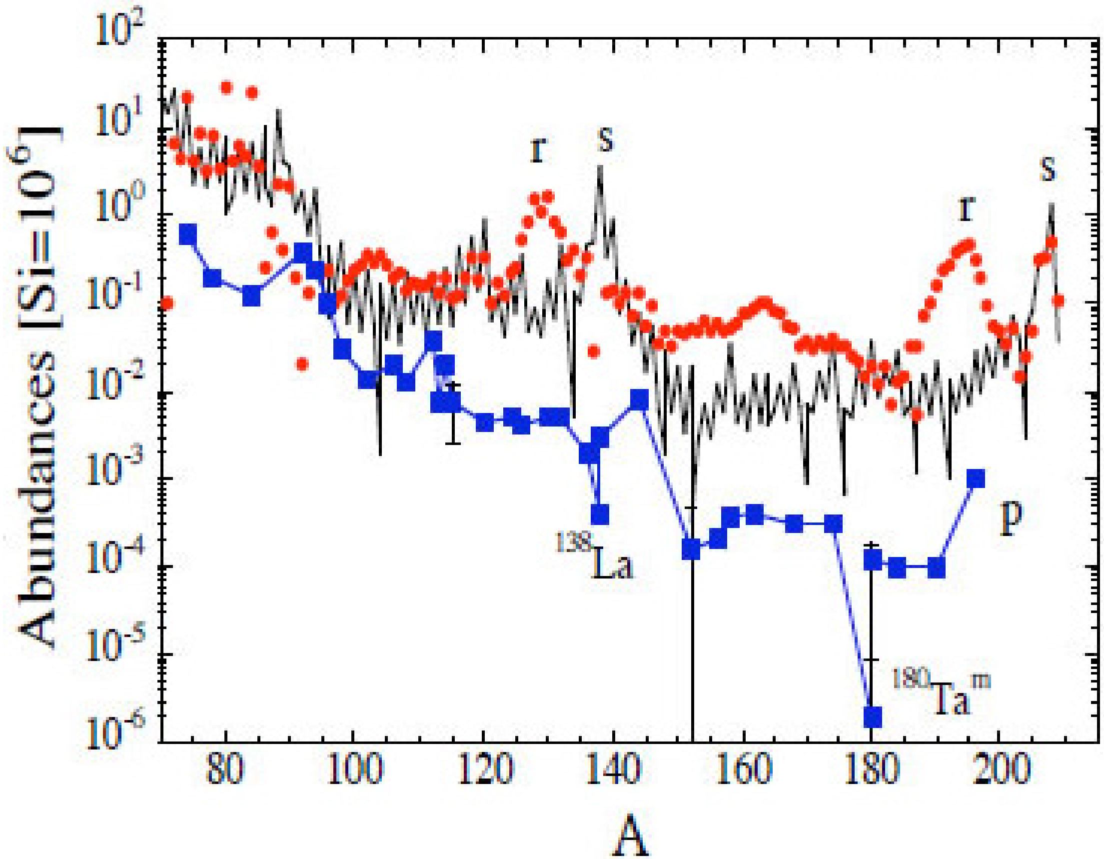

B^2FH+Cameron (1957)

H-rich layers of SNII

(p,γ) and (γ,n) reactions operating on preexisting *s*- and *r*-seed nuclei

Cameron called them '*<u>excluded isotopes</u>*'

Because of the dominant role of played by proton reactions, named these 'p-process' nuclei

They suggested temperature of the order of 2.5 10^9 K, and timescale of 10-100 s

Audouze & Truran (1975)

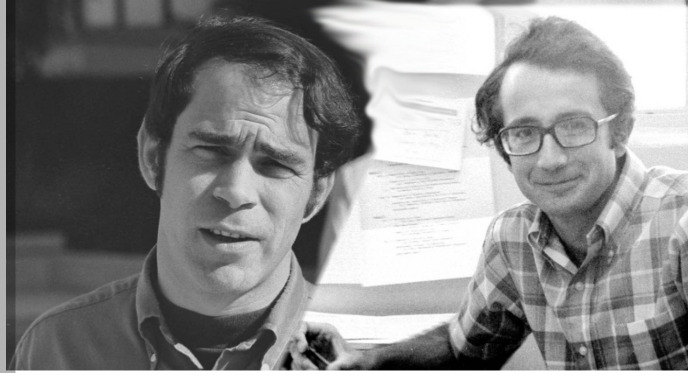

T optimum conditions for the synthesis of p-nuclei in SNII explosions: 1-2 10^9 K

H-rich matter in postshock supernova envelope following the passage of the shock wave, and realized that required T are not acquired there

Another possible site, novae associated with binary systems. In the accreted material T and ρ optimum conditions can be reached. Not sufficient matter can be produced in this site

Arnould (1976)

Synthesis of p-nuclei during hydrostatic oxygen burning

A large enhancement of heavy elements, presumably by prior *s*-processing is required. Only *s*-seed nuclei should be enhanced and not *r*-process seeds (recognized to be not important seeds).

Woosley & Howard (1978)

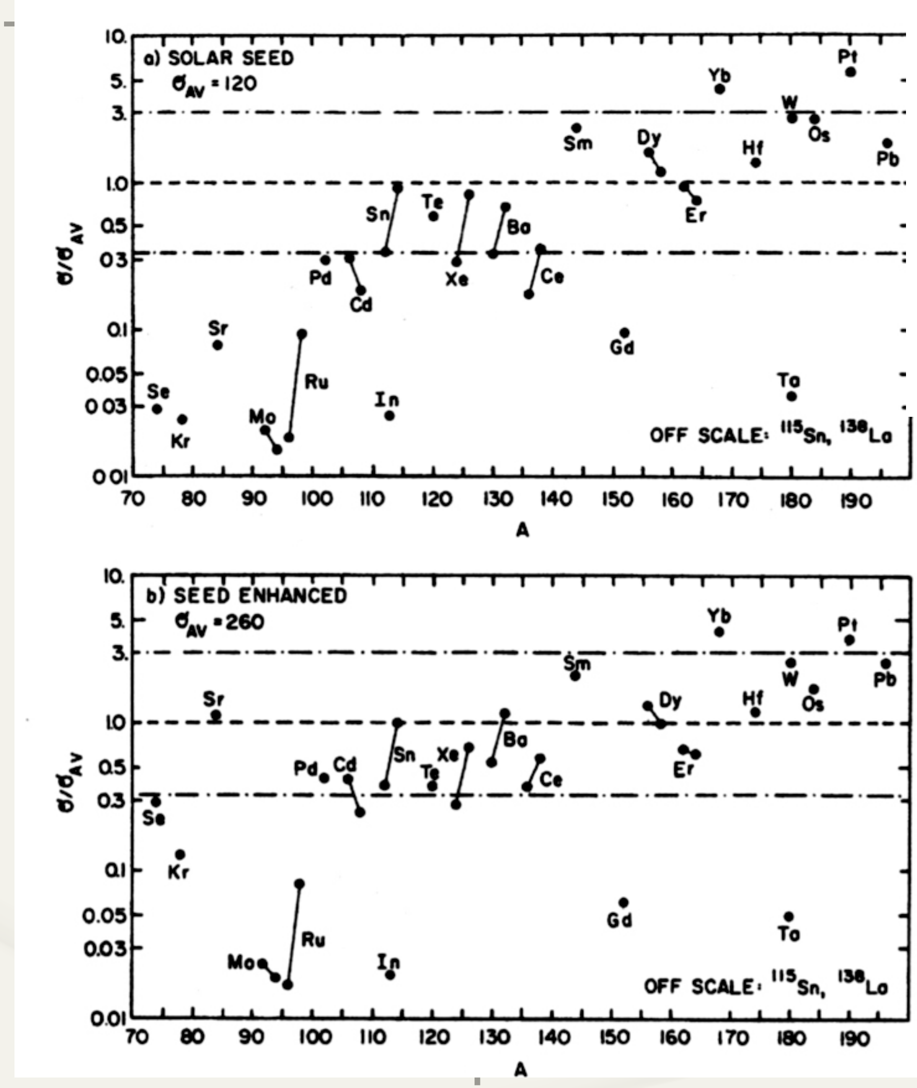

"One must still contend with disappointingly small synthesis of species like ^{92}Mo, ^{94}Mo, ^{96}Ru, ^{98}Ru"

process. A
ts subjected to
, p), (γ, α)) will
le of 1s into a
the solar

nthesis of p-
3.2 10^9 K

p-nucleosynthesis in SNII: more recent results

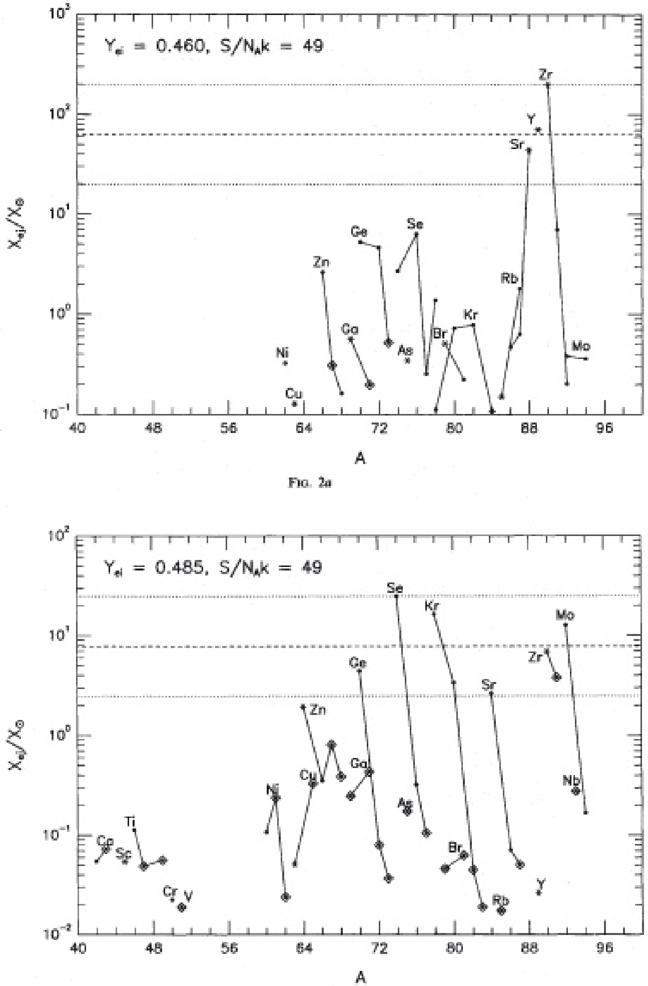

Fig. 2a

Fig. 2b

Thielemann et al., 2010

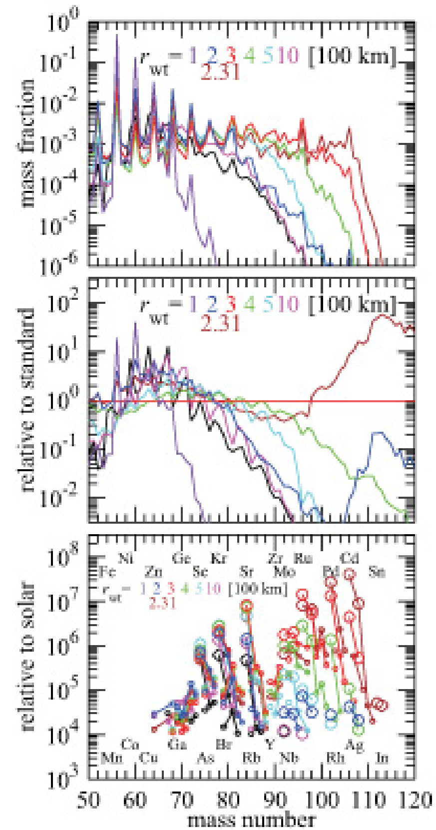

FIG. 2.— Comparison of the nucleosynthetic results for various wind-termination radii r_{wt}. The mass fractions (top) and their ratios relative to those for the standard model (middle) are shown as a function of atomic mass number. The bottom panel shows the abundances of isotopes (connected by a line for a given element) relative to their solar values, where those lower than 10^4 are omitted. The color coding corresponds to different values of r_{wt} as indicated in each panel (red is the standard model). The result for the outflow without wind termination is shown in black. In the bottom panel, the names of elements are specified in the upper (even Z) and lower (odd Z) sides at their lightest mass numbers.

This condition continues until the end of their compu-

Wanajo, Janka, Kubono 2011

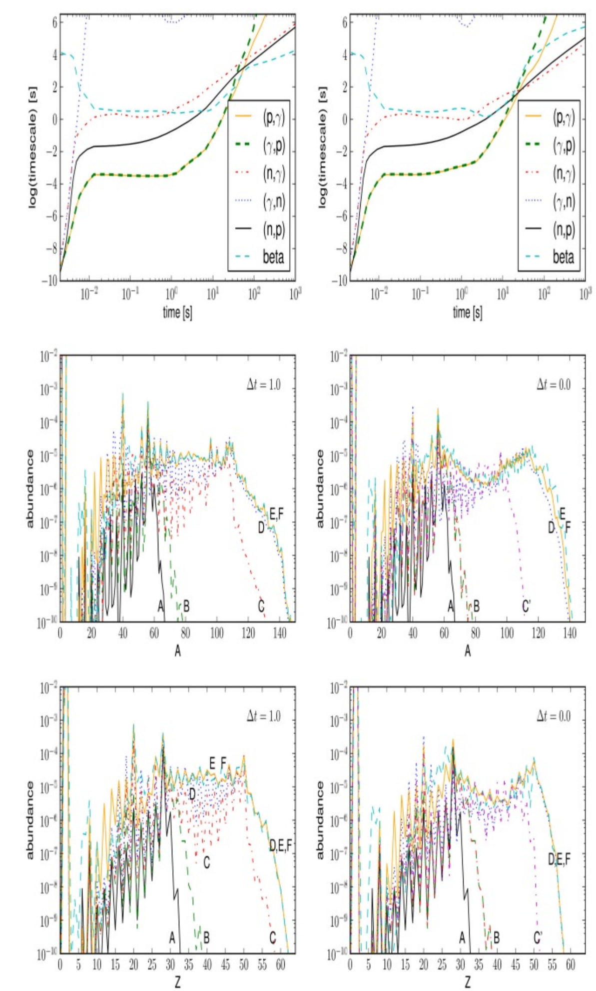

Figure 10. Left column is for the case of $\Delta t = 1.0$ s, the right column is for $\Delta t = 0.0$ s. The top row shows average timescales for different reaction types as a function of time. Abundance distributions at selected times are shown as a function of mass number (middle row) and as a function of atomic number (bottom row) for both cases of Δt. For the case $\Delta t = 1.0$ s, the abundances are shown at $T = 3.0$ (A), 2.0 (B,C), 1.6 (D), 1.0 GK (E), and also the final abundances (F). The abundances at the beginning (B) and at the end (C) of the constant temperature phase differ quite significantly. For the case $\Delta t = 0.0$ s, the abundances are shown at $T = 3.0$ (A), 2.0 (B), 1.9 (C′), 1.5 (D), 1.0 GK (E) and also the final abundances (F). Note that while the abundances at C for $\Delta t = 1.0$ s and at C′ for $\Delta t = 0.0$ s are similar, the temperature is slightly lower for C′ because there is no constant temperature phase in this case.

(A color version of this figure is available in the online journal.)

Arcones et al. 2012

Howard, Meyer & Woosley (1991)

A new site for the gamma-process: Type Ia supernovae. CO-WD that explodes by deflagration or detonation.

They investigate chains to produce the light-p, and found that

^{86}Kr(p,γ) … ^{90}Zr(p,γ)^{91}Nb(p,γ)^{92}Mo

is responsible for half of ^{92}Mo (and important for ^{90}Zr as well) and (p,γ) reactions produce also ^{96}Ru. The other half of ^{92}Mo, and ^{94}Mo, come from (γ,n) reaction sequence

Goriely et al. (2002, 2005)

He accreting WD with sub-Chandrasekhar mass

p-process are produced in the accreting He-layers

Tested different initial abundances of s-nuclei, up to 100xsolar

They found that most of the p-nuclei are coproduced at level close to solar, but underproduced (except ^{78}Kr) with respect to Fe

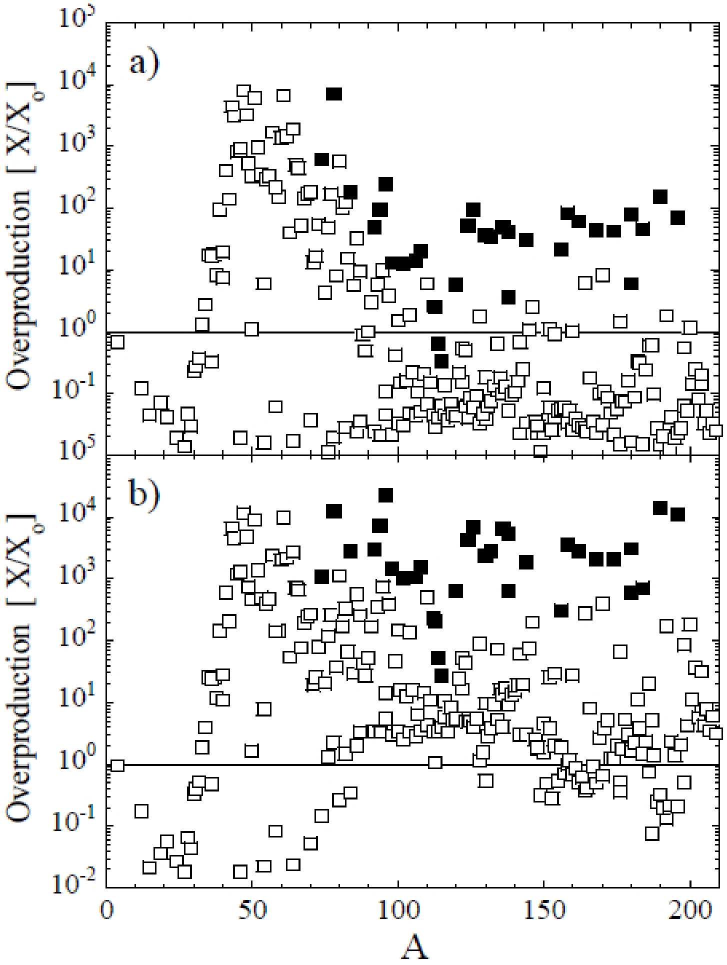

Kusakabe,Iwamoto & Nomoto (2011)

They used as SNIa model the W7 (Nomoto et al.'84), pure deflagration

They also examine the impact of different s-seed distributions

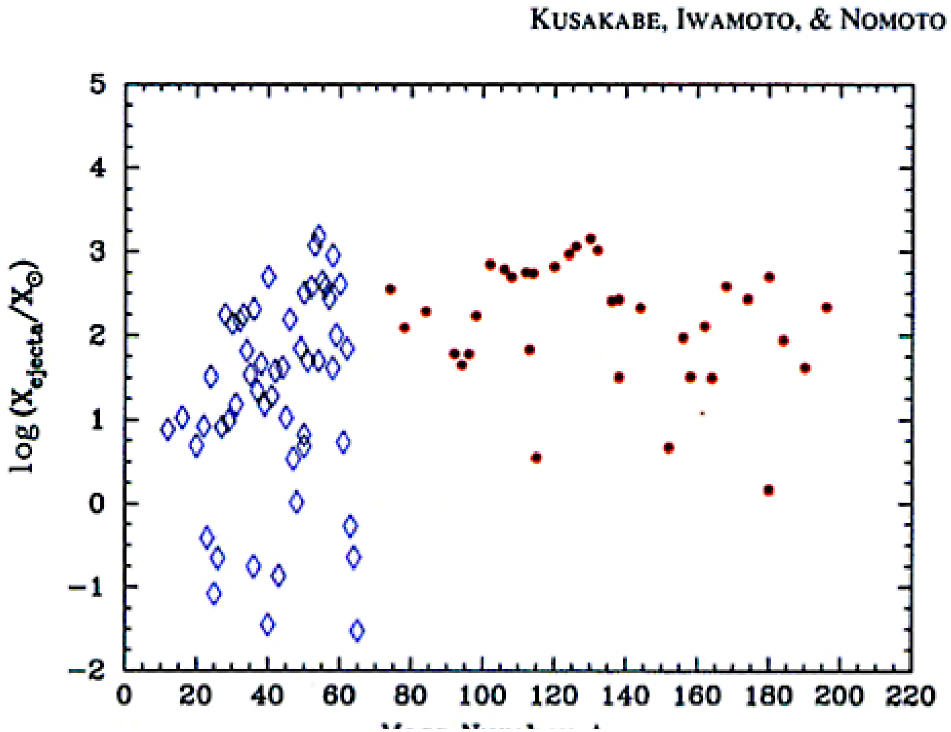

Travaglio et al. 2011, *ApJ 739,93*

F. Roepke & W.Hillebtandt

SNIa models

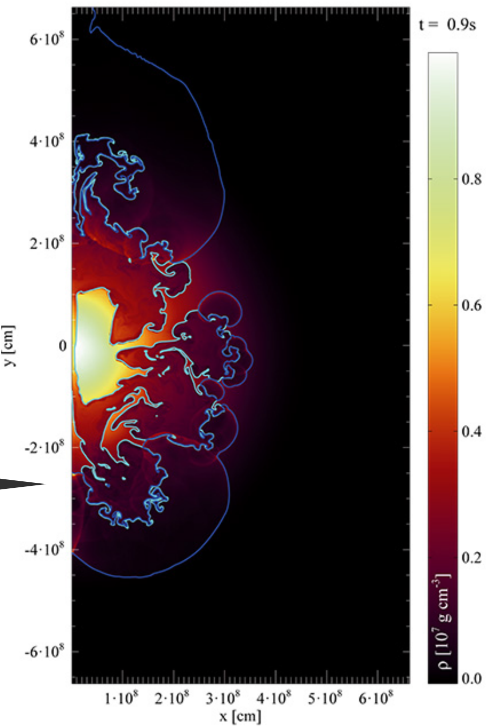

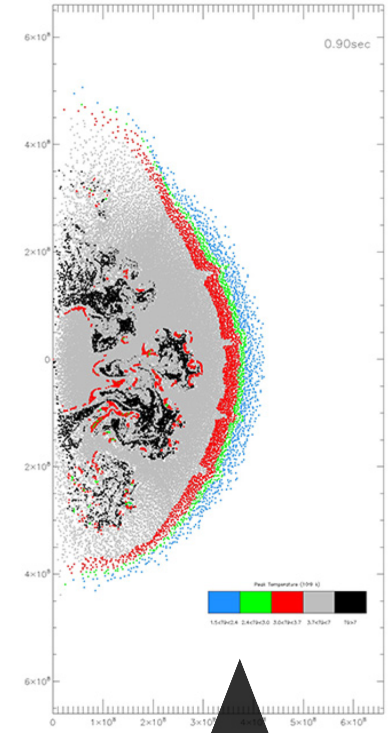

C. Travaglio

p-process nucleosynthesis

R. Gallino

s-process seeds

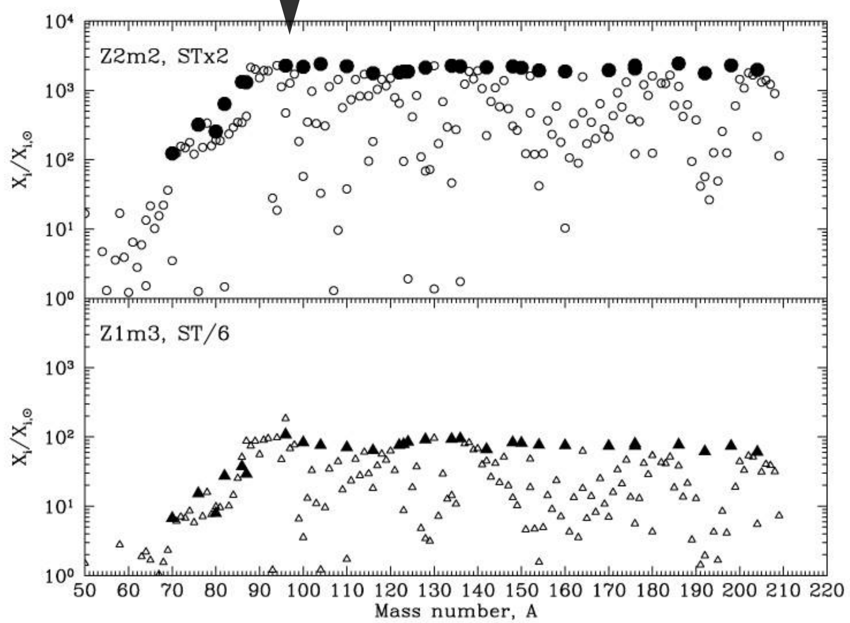

s-process in accreted matter

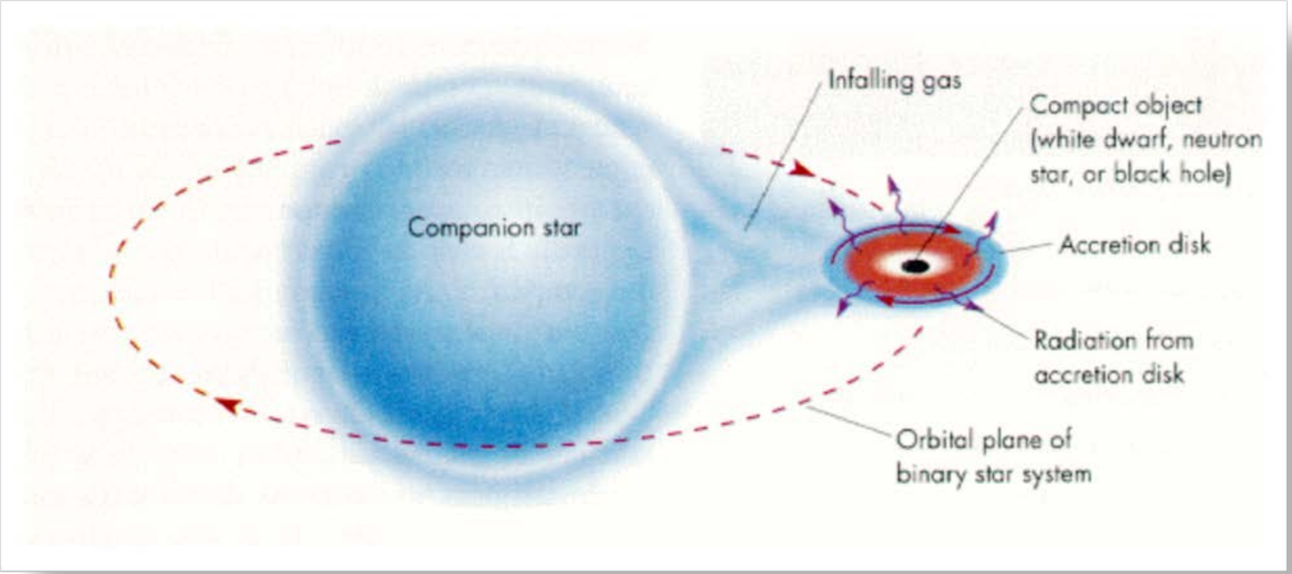

"Accreting white dwarfs as an alternate or additional source of s-process isotopes" (Iben, ApJ 243, 1981)

H-accreting CO white

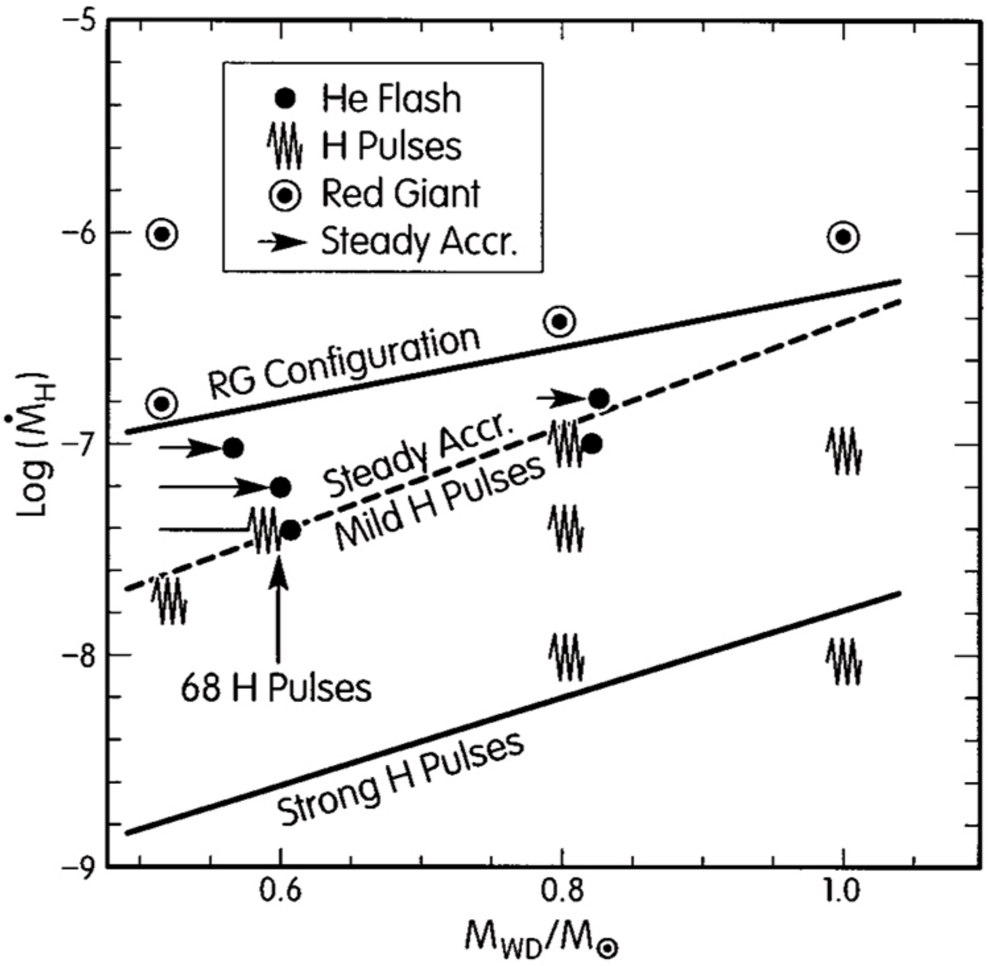

FIG. 10.—Parameter space in the $\dot{M}$-M_{WD} plane explored in the present work. Various symbols mark the different outcomes experienced by the various computed models, depending on initial white dwarf mass and accretion rate (see the text for symbol meanings). The results of accretion experiments performed by Livio et al. (1989) with a 1 $M_\odot$ WD are also shown at the right in the figure.

Cassisi, Iben, Tornambe' 1998, ApJ, 496, 376

Piersanti, Cassisi, Iben, Tornambe' 2000, ApJ, 535, 932

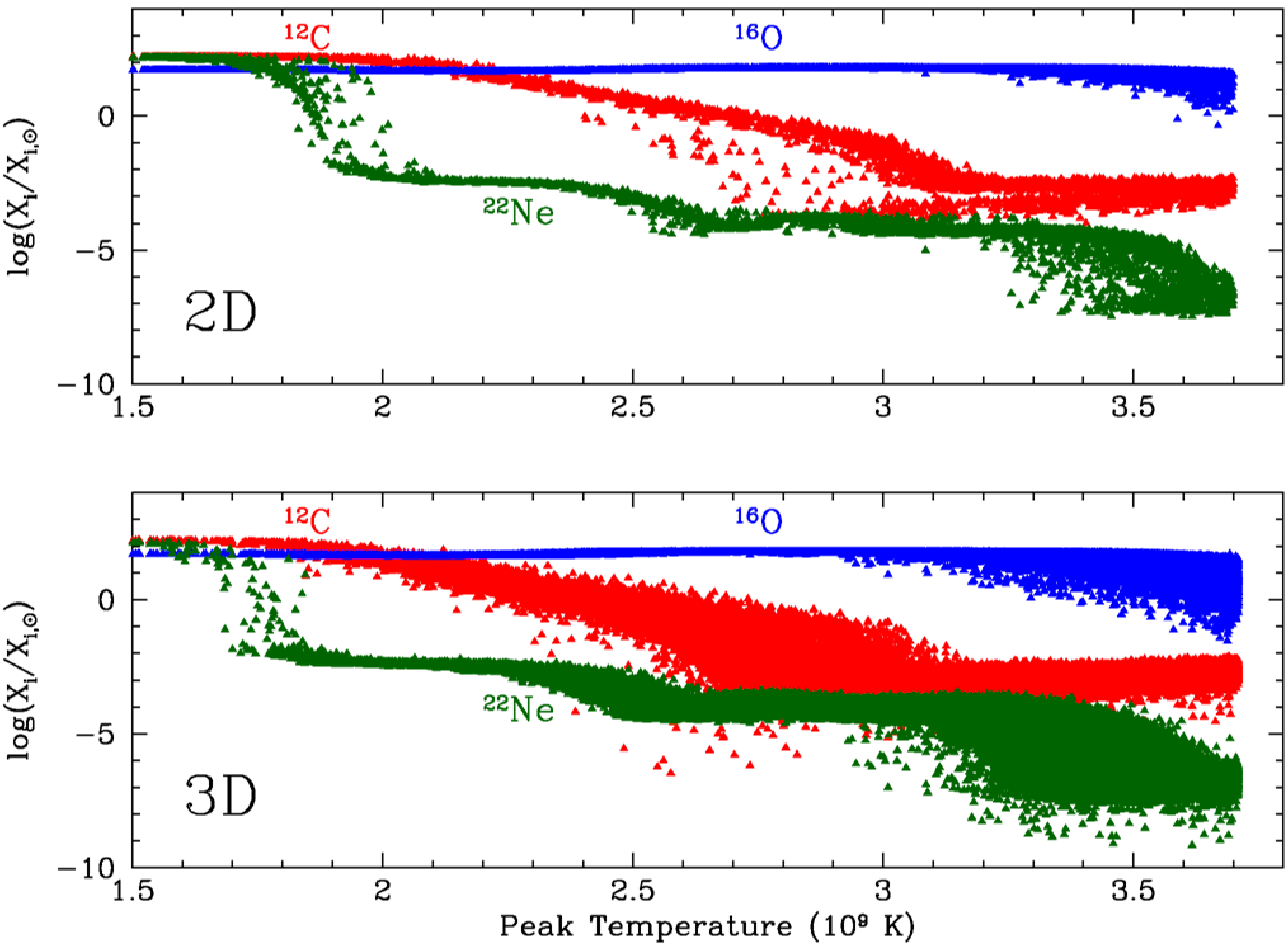

12C
16O
22Ne
2D
log(Xi/Xi,⊙)
0
−5
−10
1.5
2
2.5
3
3.5
12C
16O
22Ne
3D
log(Xi/Xi,⊙)
0
−5
−10
1.5
2
2.5
3
3.5
Peak Temperature (10⁹ K)

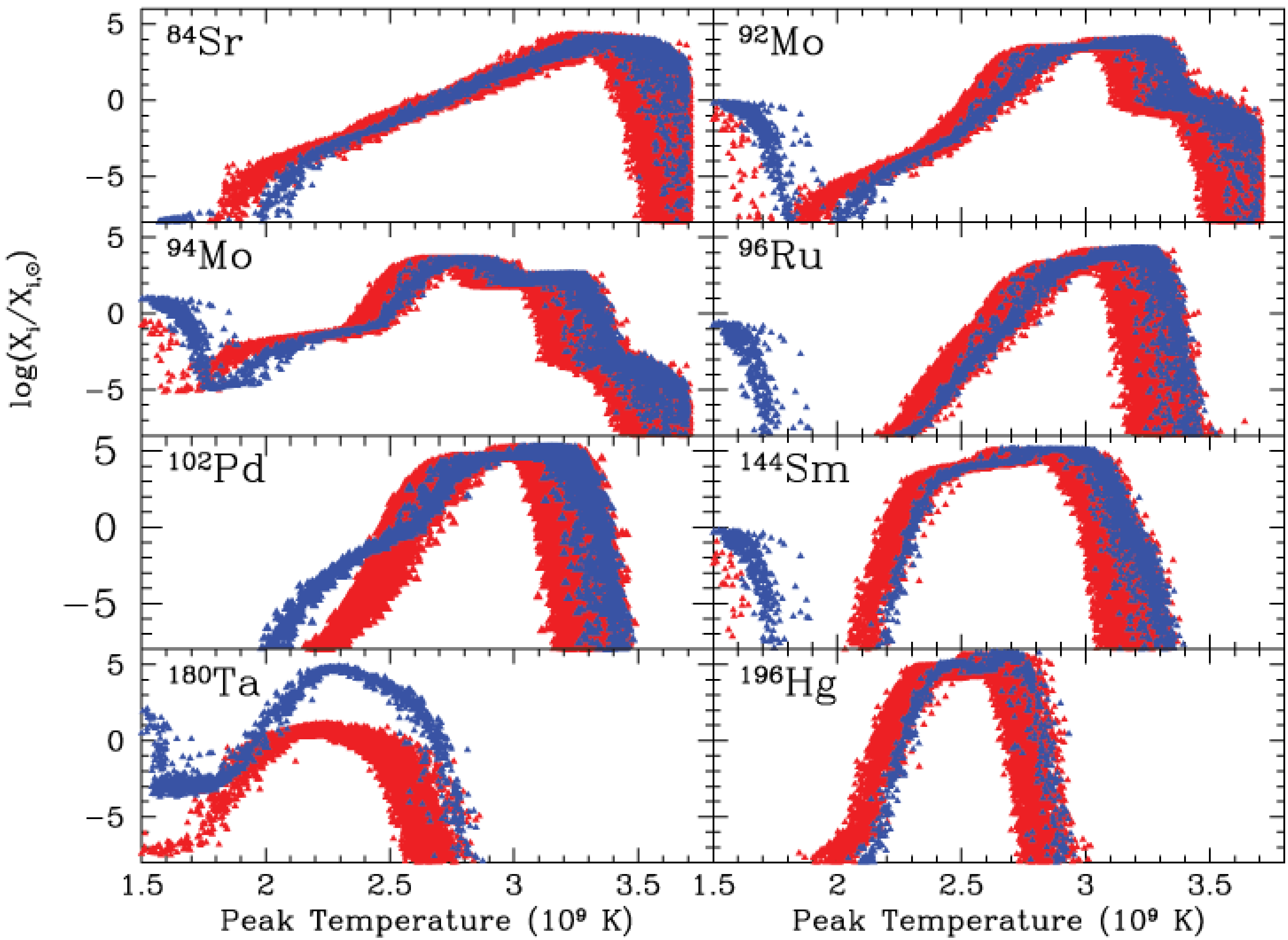

^{84}Sr
^{92}Mo
^{94}Mo
^{96}Ru
^{102}Pd
^{144}Sm
^{180}Ta
^{196}Hg
log(X$_i$/X$_{i,\odot}$)
5
0
−5
1.5
2
2.5
3
3.5
Peak Temperature (10^9 K)

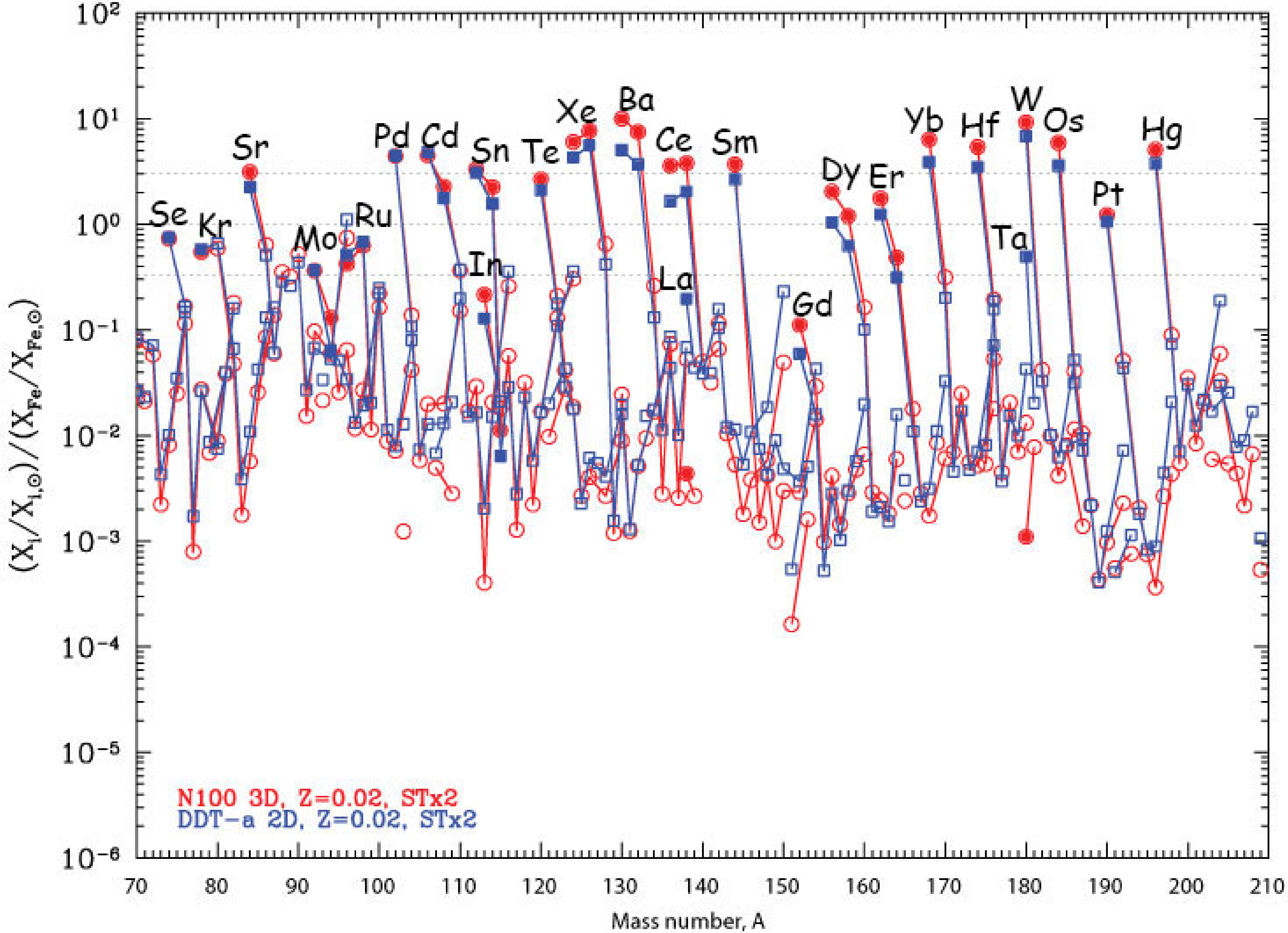

Se
Kr
Sr
Mo
Ru
Pd
Cd
In
Sn
Te
Xe
Ba
Ce
La
Sm
Gd
Dy
Er
Yb
Hf
Ta
W
Os
Pt
Hg
N100 3D, Z=0.02, STx2
DDT-a 2D, Z=0.02, STx2
$(X_i/X_{i,\odot})/(X_{Fe}/X_{Fe,\odot})$
Mass number, A

NO p-isotopes

^{113}In, ^{115}Sn are p-only isotopes?
r-process contribution *(Dillmann et al. 2008, Nemeth et al. 1994)*?

^{138}La produced by neutrino
(Woosley et al. 1990)

^{152}Gd and ^{164}Er large s-process contribution
at solar composition
(Arlandini et al. 1999, Kaeppeler et al. 2011)

^{180}Ta at least 50% contribution
from s-process at solar composition
(Mohr et al. 2007)

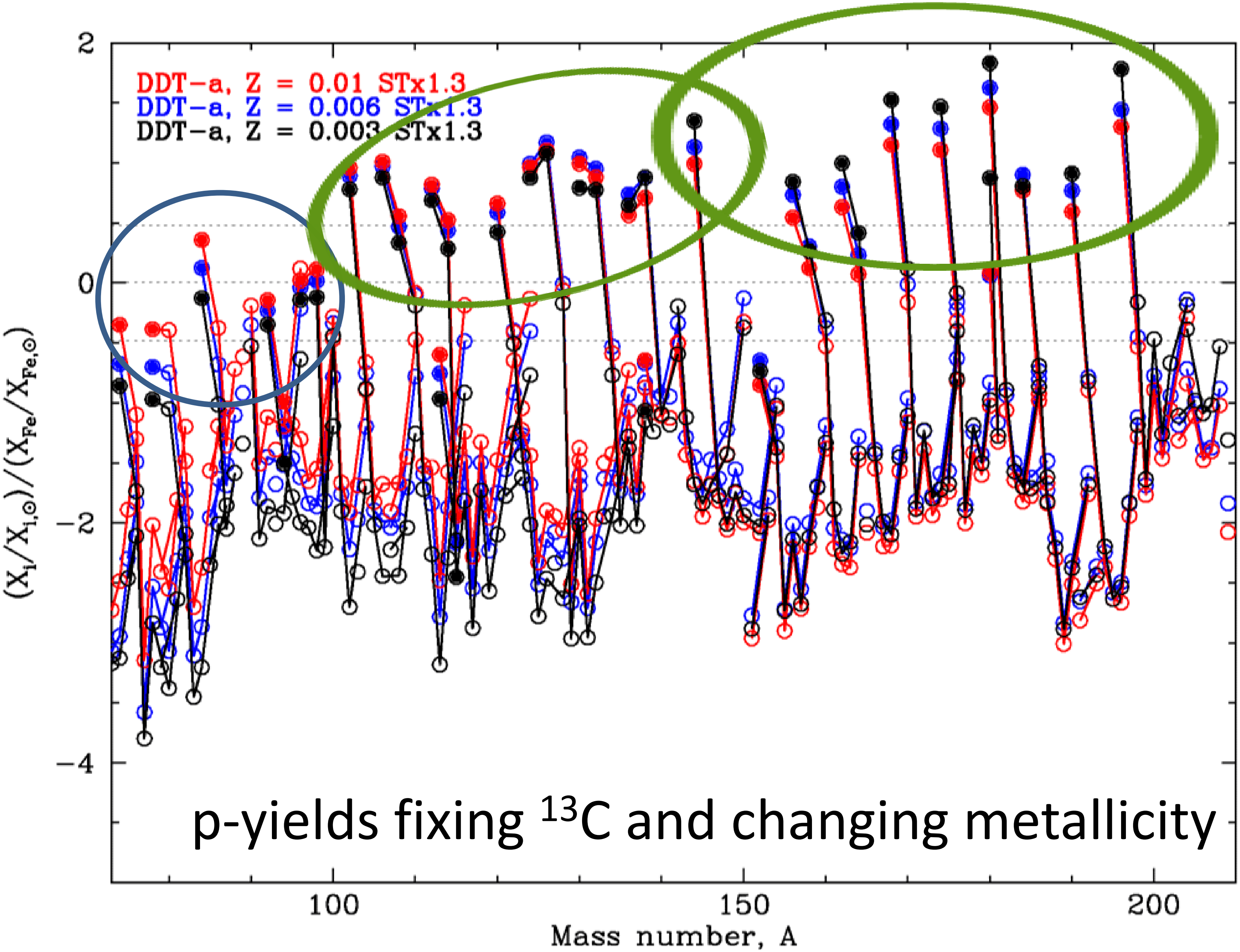
DDT-a, Z = 0.01 STx1.3
DDT-a, Z = 0.006 STx1.3
DDT-a, Z = 0.003 STx1.3
p-yields fixing ^{13}C and changing metallicity
$(X_i/X_{i,\odot})/(X_{Fe}/X_{Fe,\odot})$
Mass number, A
2
0
−2
−4
100
150
200

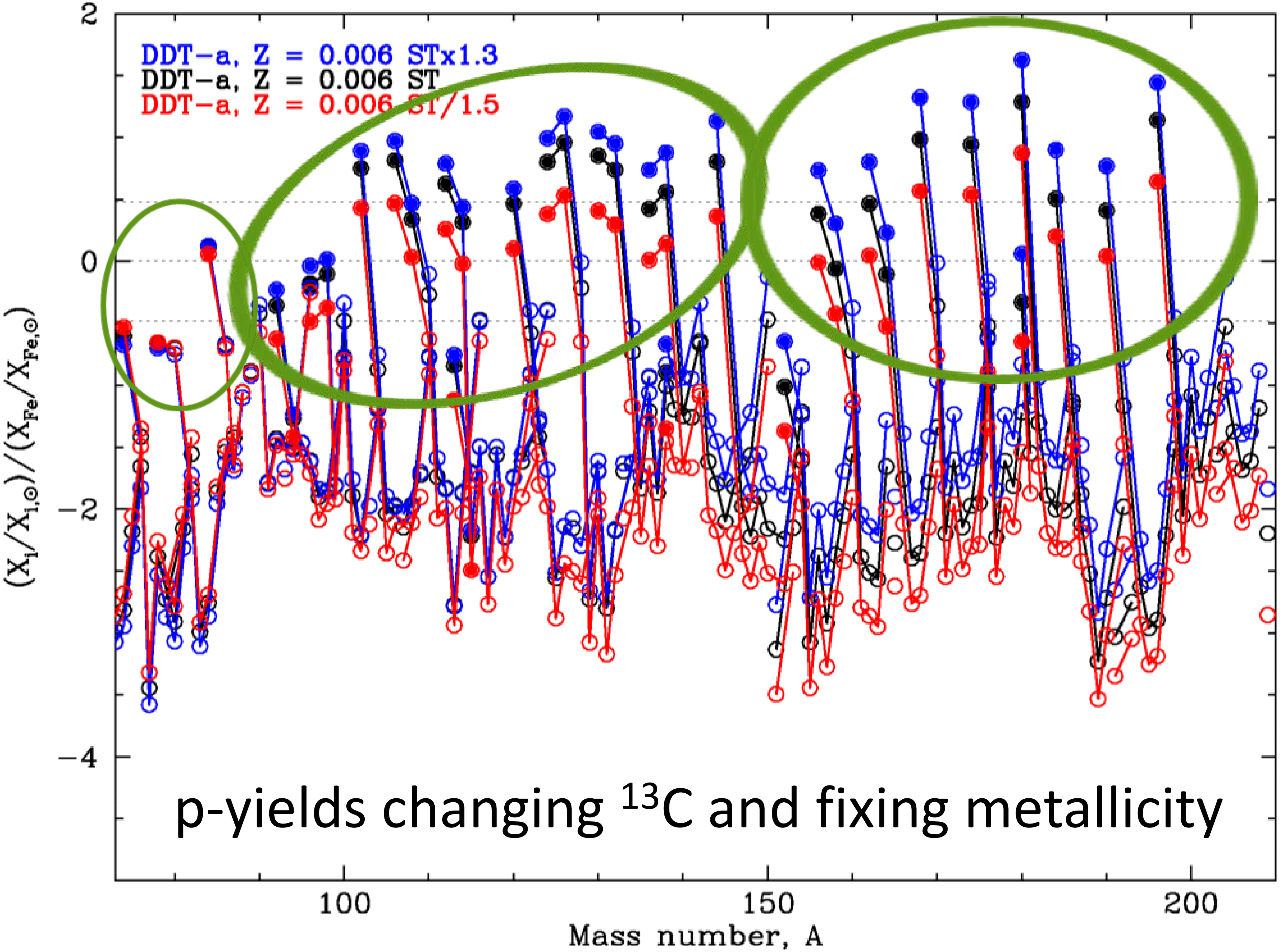
DDT-a, Z = 0.006 STx1.3
DDT-a, Z = 0.006 ST
DDT-a, Z = 0.006 ST/1.5
2
0
−2
−4
100
150
200
Mass number, A
$(X_i/X_{i,\odot})/(X_{Fe}/X_{Fe,\odot})$
p-yields changing ^{13}C and fixing metallicity

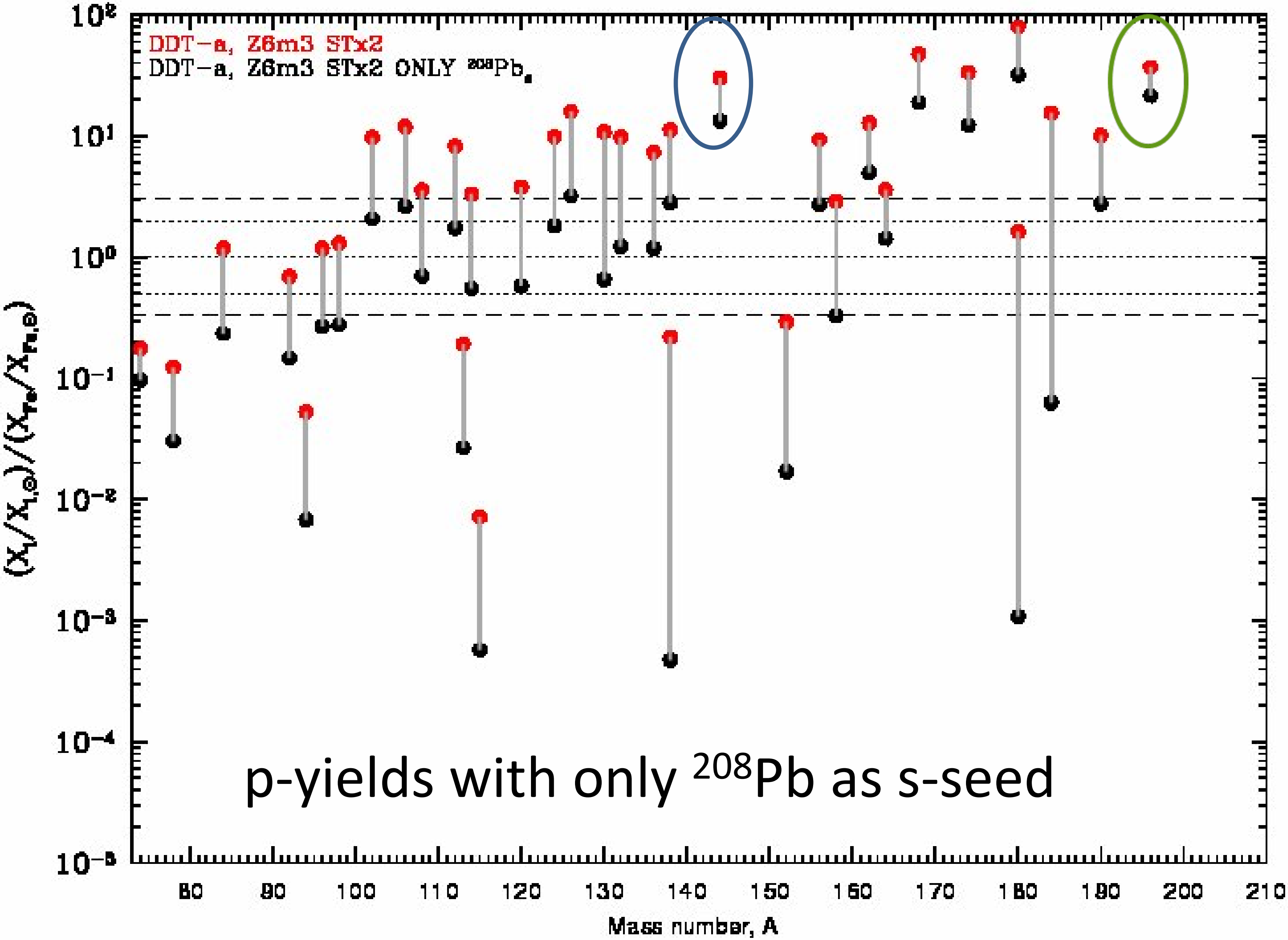
DDT-a, Z6m3 STx2
DDT-a, Z6m3 STx2 ONLY 208Pb
p-yields with only 208Pb as s-seed
(X_i/X_i,⊙)/(X_Fe/X_Fe,⊙)
10^2
10^1
10^0
10^-1
10^-2
10^-3
10^-4
10^-5
80
90
100
110
120
130
140
150
160
170
180
190
200
210
Mass number, A

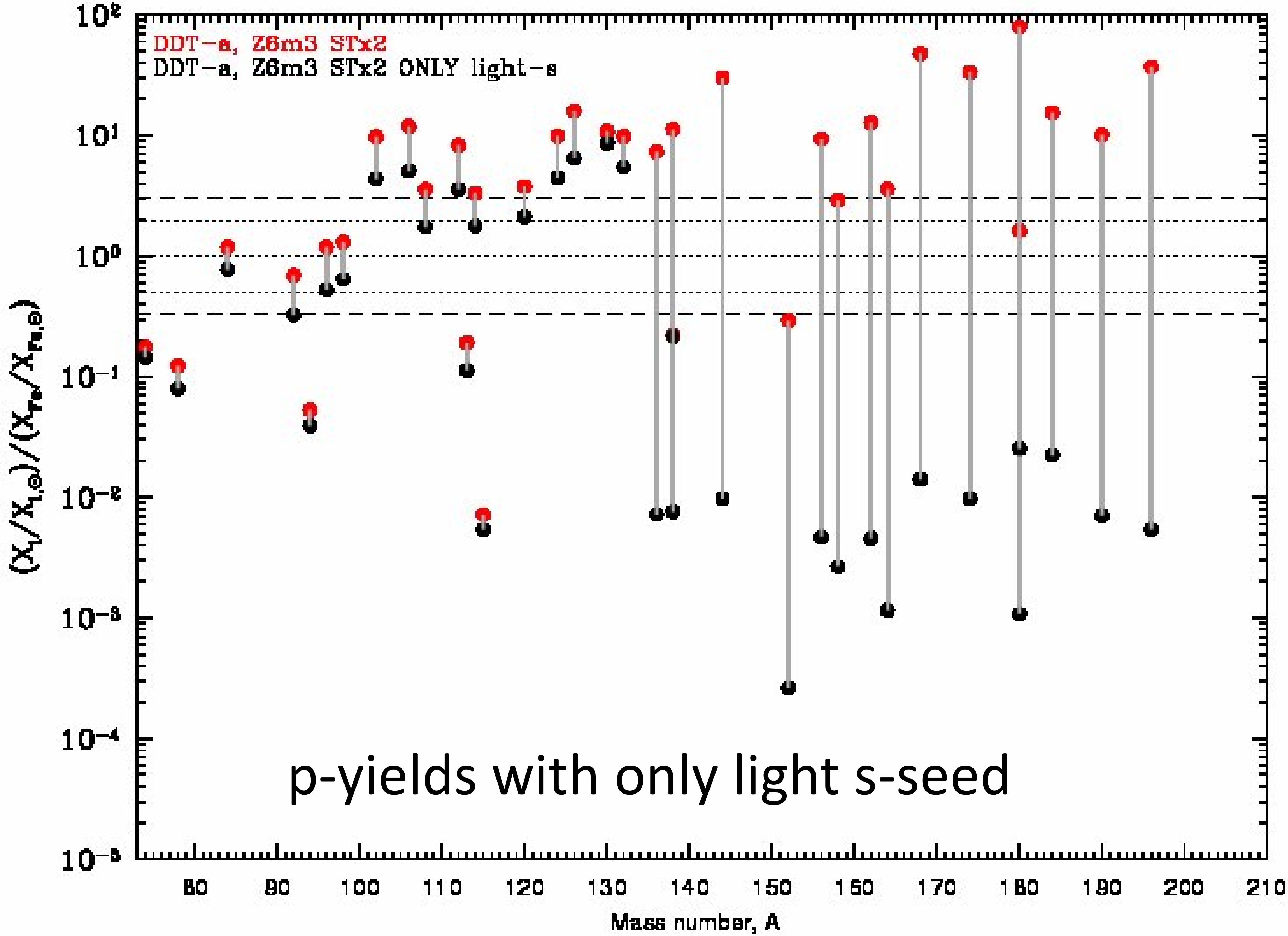

DDT-a, Z6m3 STx2
DDT-a, Z6m3 STx2 ONLY light-s
p-yields with only light s-seed
(X_i/X_i,⊙)/(X_Fe/X_Fe,⊙)
10^2
10^1
10^0
10^-1
10^-2
10^-3
10^-4
10^-5
80
90
100
110
120
130
140
150
160
170
180
190
200
210
Mass number, A

Galactic chemical evolution code (Travaglio et al. 2004)

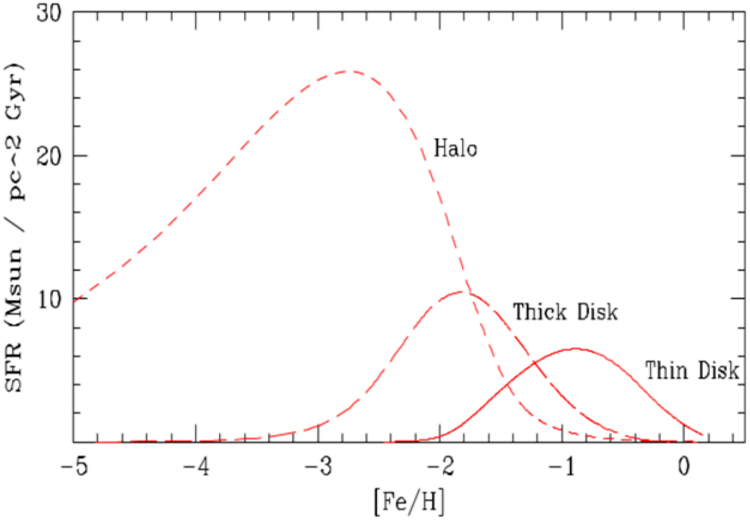

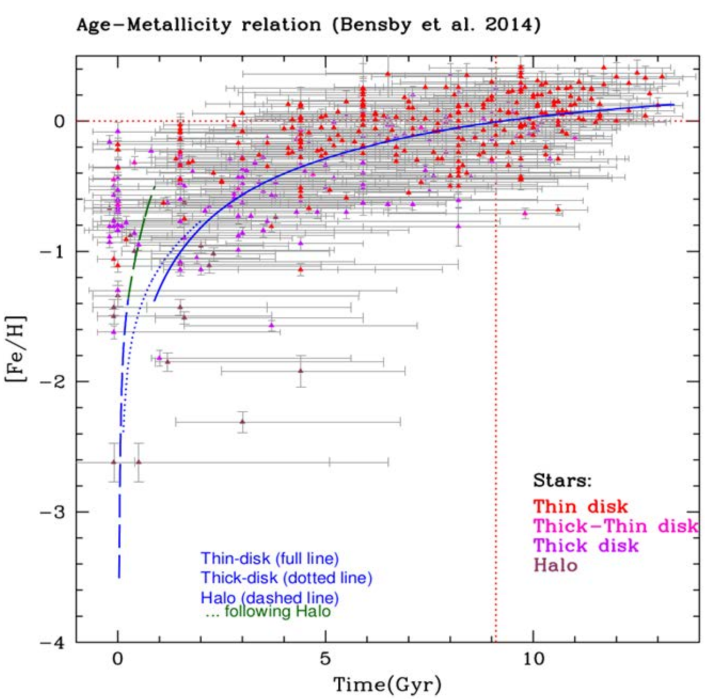

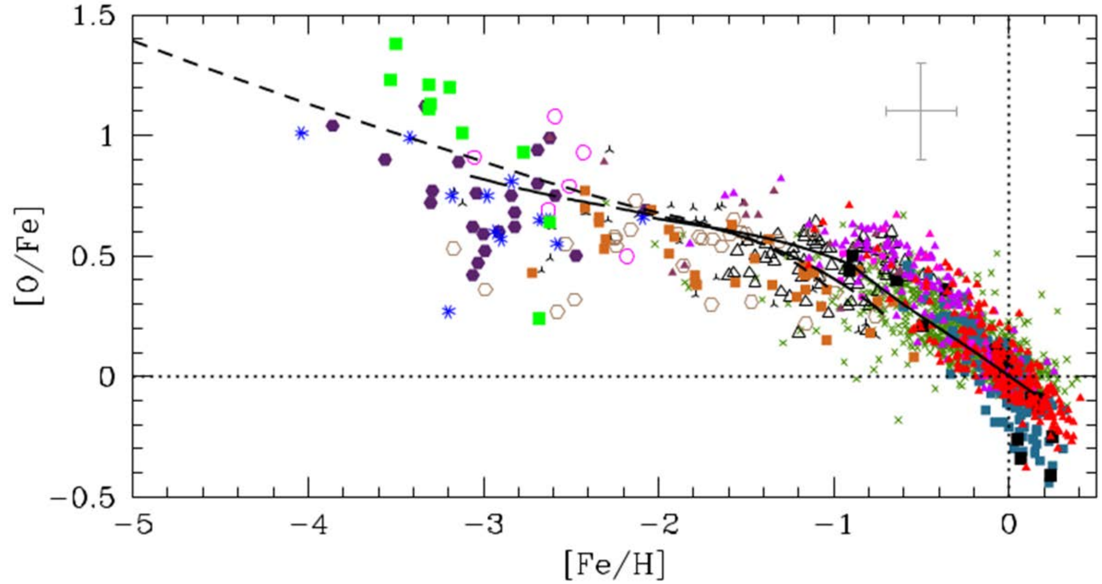

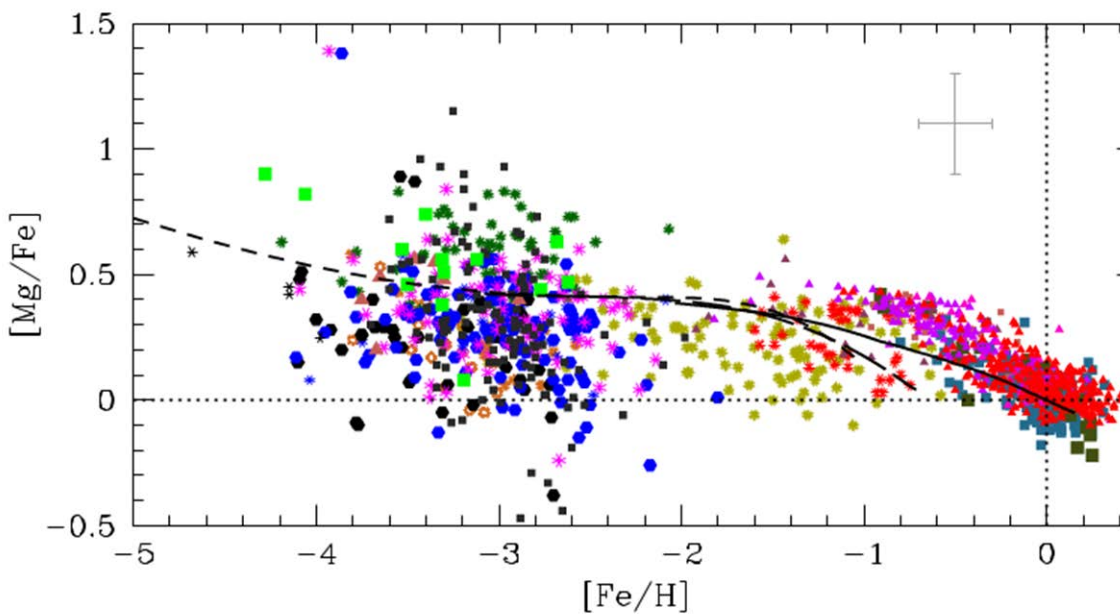

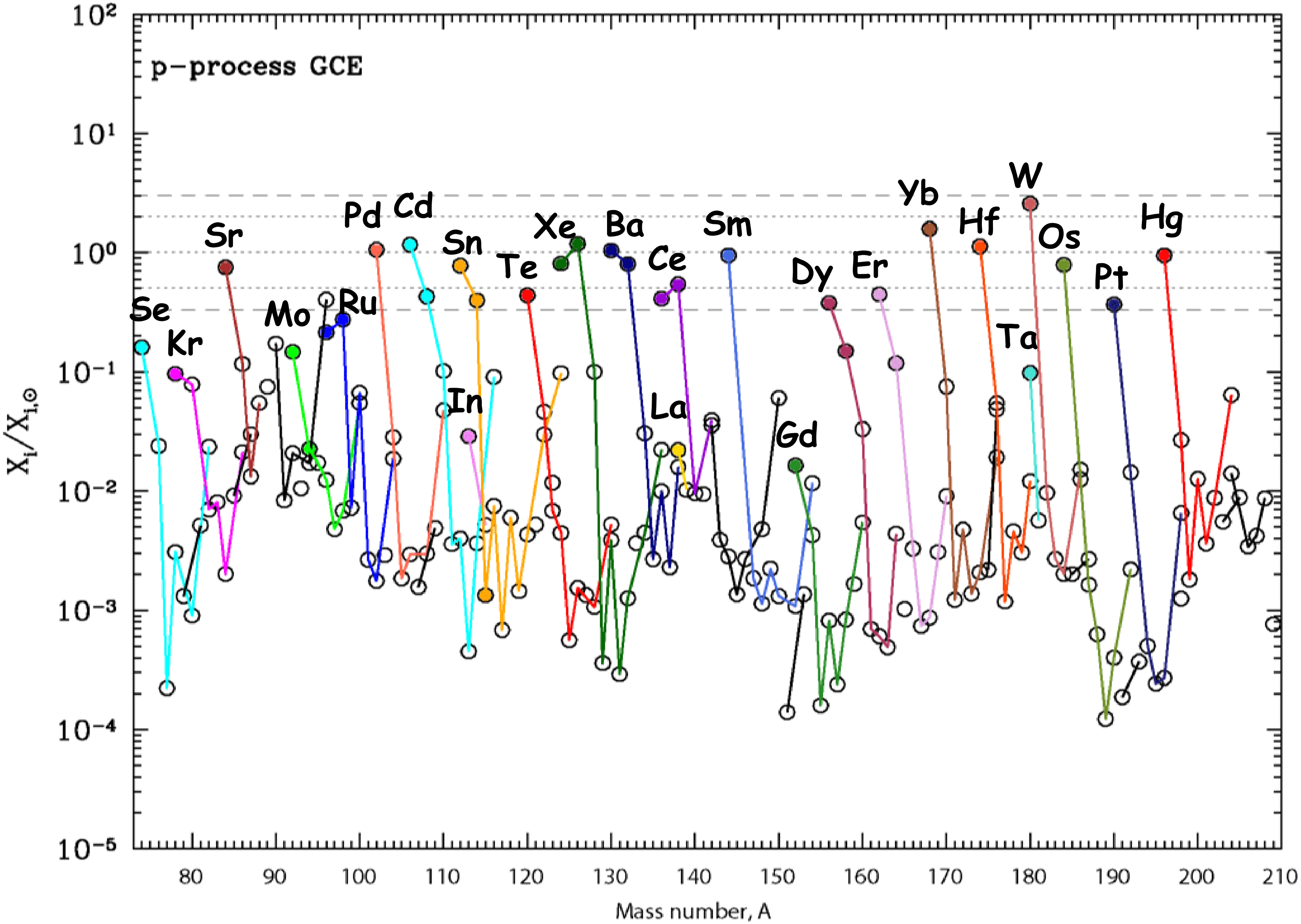

Galactic chemical evolution

(Travaglio et al. 2014, ApJ submitted)

Radiogenic p-isotopes ^{92}Nb and ^{146}Sm in SNIa

	Meteorite	GCE
$^{92}Nb/^{92}Mo$	$(2.8 \pm 0.5)\times10^{-5}$	3.3×10^{-5}

Uncertainties for $^{90}Zr(p,\gamma)^{91}Nb/2$, $^{91}Nb(n,\gamma)^{92}Nb\times2$ $^{92}Nb(n,\gamma)^{93}Nb/2$

	Meteorite	GCE
$^{146}Sm/^{144}Sm$	$(9.4 \pm 0.5)\times10^{-3}$	1.7×10^{-2}

Rauscher et al. (2013), new $^{148}Gd(\gamma,\alpha)^{144}Sm$ rate

Travaglio et al. (2014, ApJ in press)

Future directions

- Analysis of all p-isotopes production/destruction channels (in collaboration with K. Göbel, R. Reifarth) and related nuclear uncertainties (see this afternoon discussion for light p-nuclei analysis)

- More detailed analysis on 3D models (in collaboration with I. Seitenzahl)

- Different SNIa: mergers, sub-Ch (in collaboration with F. Röpke)

Light-p production/destruction channels in SNIa and nuclear uncertainties
(afternoon discussion)

Travaglio C. (INAF-Astrophysical Observatory Turin,Italy)

COLLABORATORS:

Gallino R.,

Röpke F., Seitenzahl I., Hillebrandt W.,

Rauscher T., Reifarth R., Göbel K.,

Dauphas N.

COMPUTER RESOURCES: B2FH Ricerca per l'Astrofisica Nucleare; GOETHE UNIVERSITÄT FRANKFURT AM MAIN

Reaction libraries and codes comparison

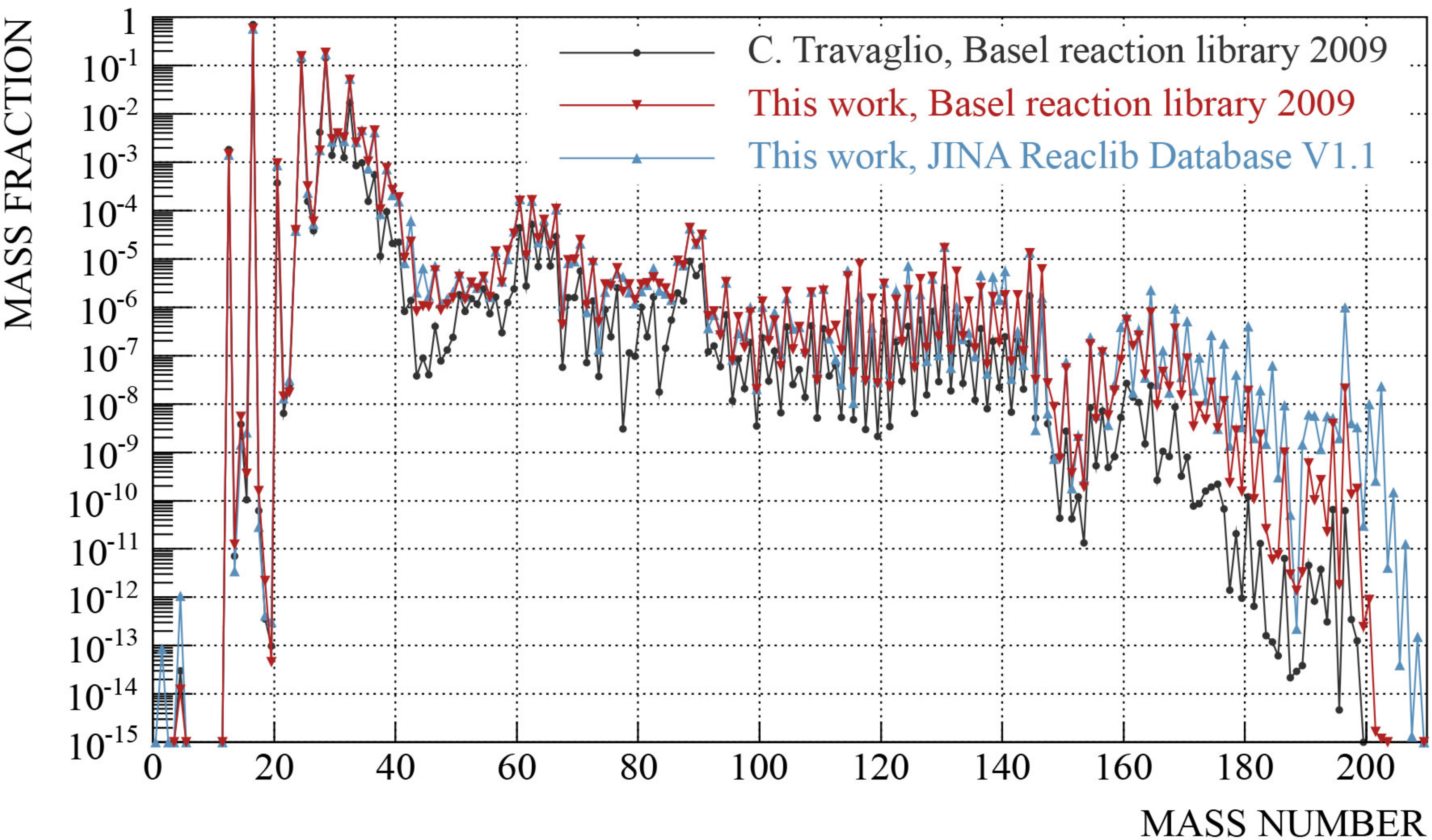

Light p-nuclei

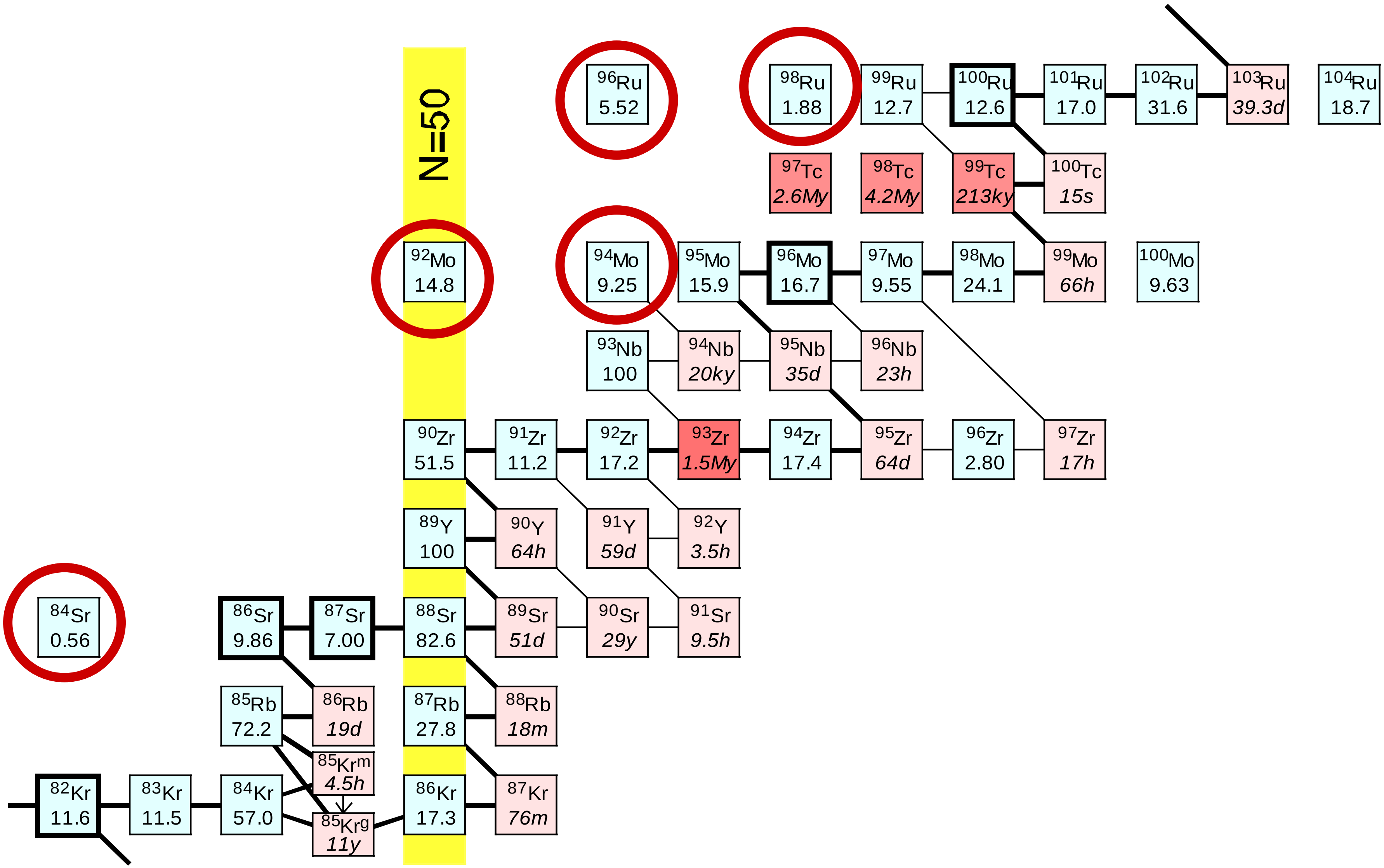

Mo isotopes

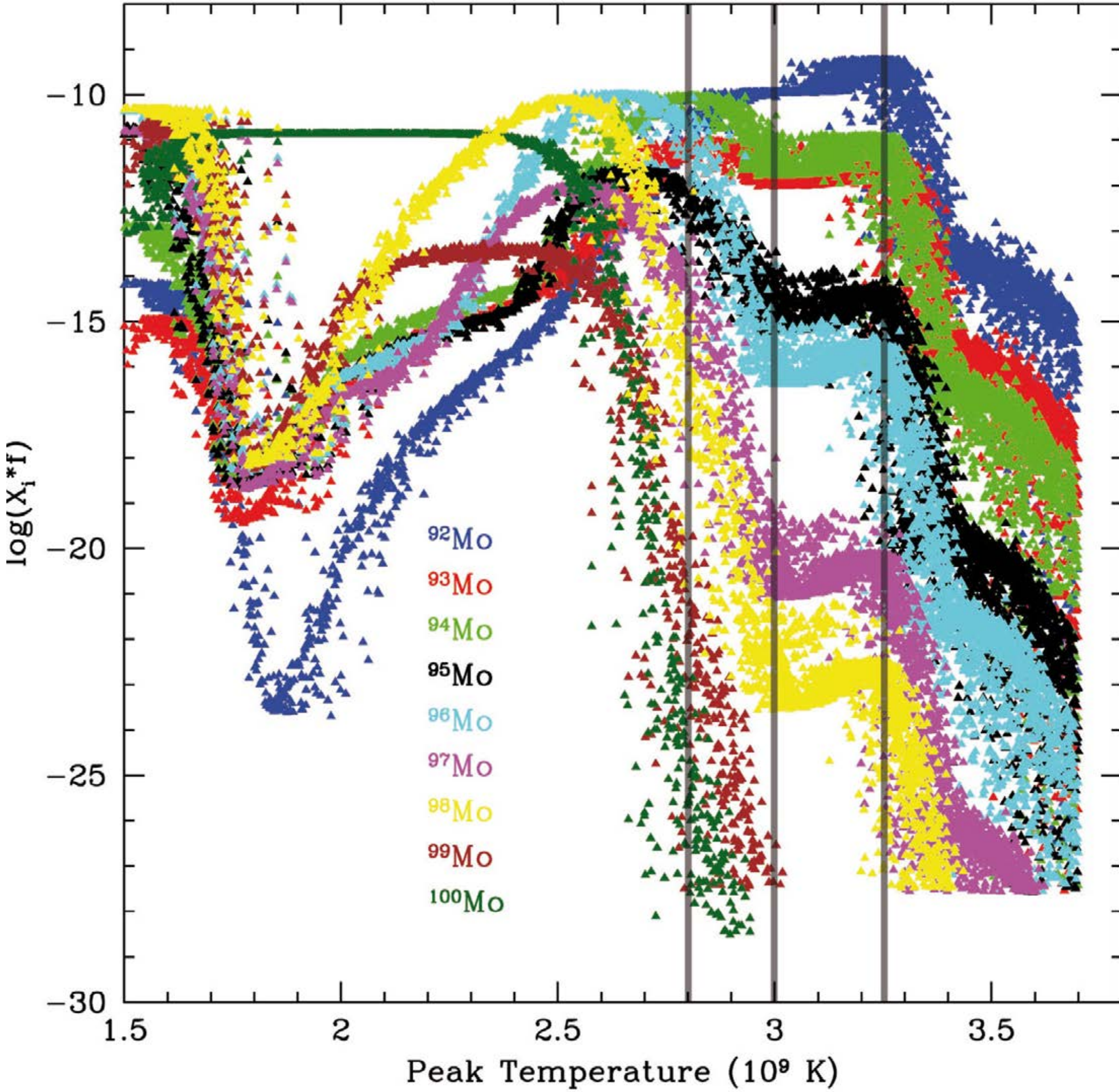

log(X_i*f)
−10
−15
−20
−25
−30
1.5
2
2.5
3
3.5
Peak Temperature (10⁹ K)
⁹²Mo
⁹³Mo
⁹⁴Mo
⁹⁵Mo
⁹⁶Mo
⁹⁷Mo
⁹⁸Mo
⁹⁹Mo
¹⁰⁰Mo

Tracer	Abundance study	T_{max} (GK)	Comment
1	^{92}Mo	3.2	maximum abundance of ^{92}Mo
2	^{92}Mo	3.2	minimum abundance of ^{92}Mo
3	^{94}Mo	2.8	maximum abundance of ^{94}Mo
4	^{94}Mo	2.8	minimum abundance of ^{94}Mo
5	^{94}Mo	3.0	abundance of ^{94}Mo drops for tracers with $T_{max} \gtrsim 3.0$ GK

Table 4.2.: Tracers selected for the PPN simulations using a Supernova type Ia model.

^{92}Mo

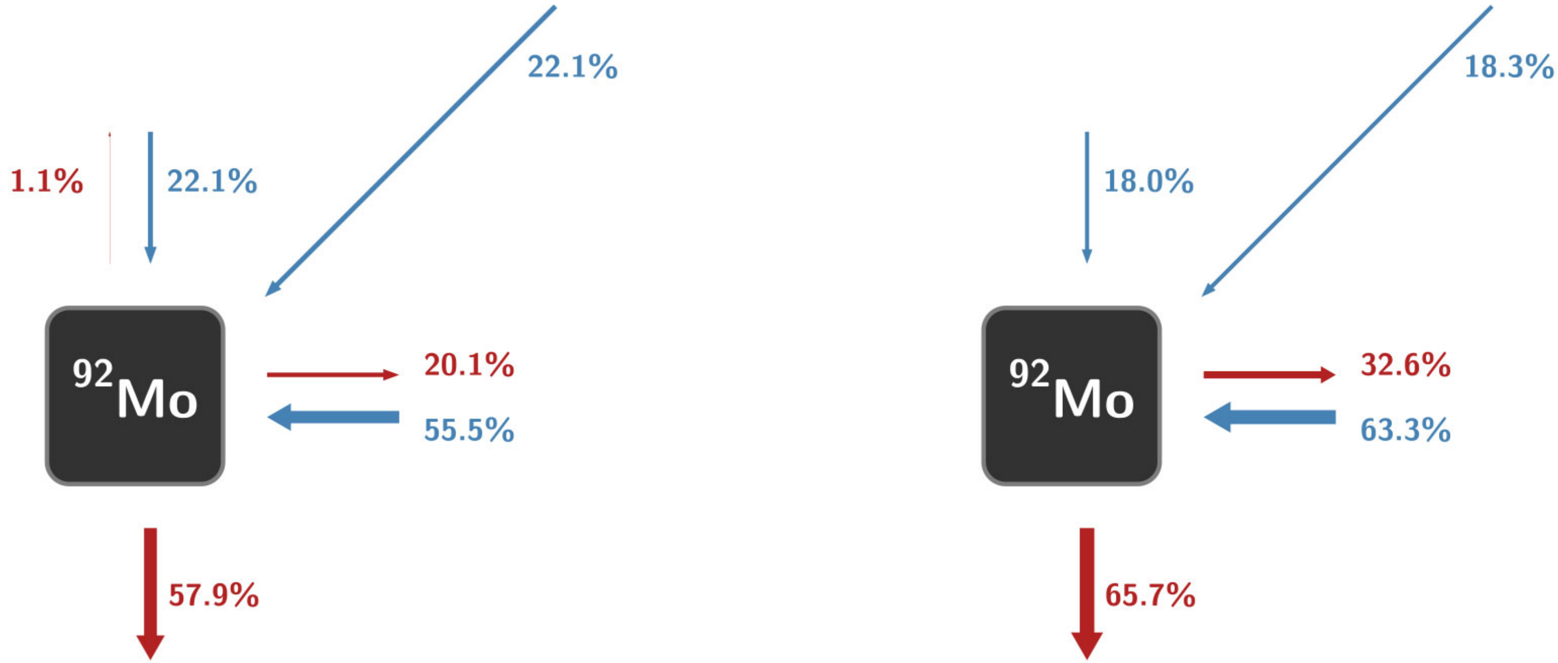

(a) Tracer-1.

(b) Tracer-2.

^{94}Mo

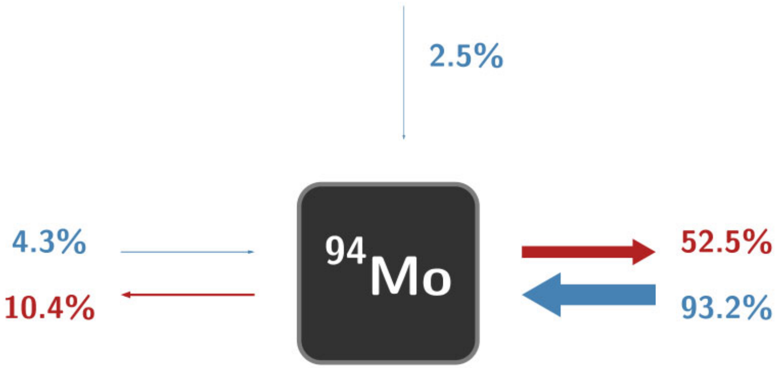

(a) Tracer-3.

(b) Tracer-4.

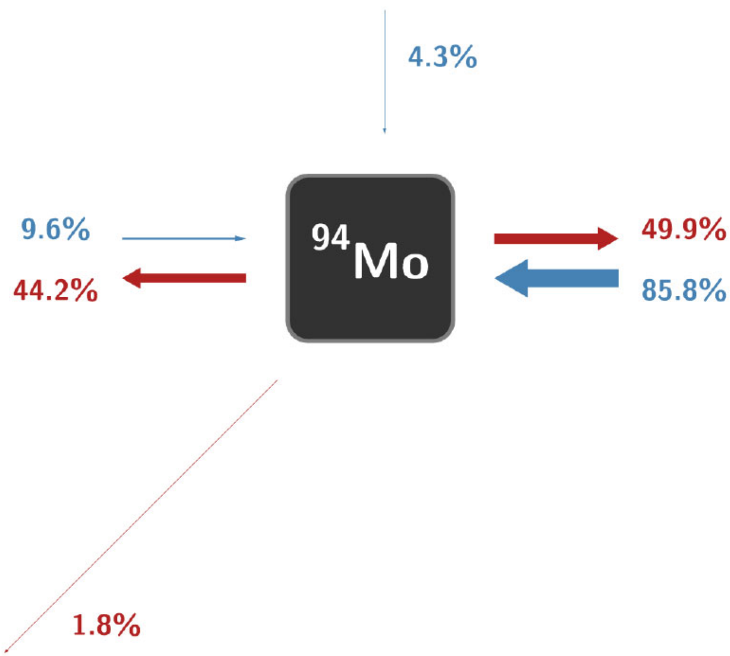

Radiogenic p-isotopes ^{92}Nb and ^{146}Sm in SNIa

	Meteorite
$^{92}Nb/^{92}Mo$	$(2.8 \pm 0.5)\times10^{-5}$
$^{146}Sm/^{144}Sm$	$(9.4 \pm 0.5)\times10^{-3}$

^{146}Sm/^{144}Sm in SNII: dependence on ^{144}Sm(α,γ)^{148}Gd rate

TABLE I. Stellar ^{144}Sm(α,γ)^{148}Gd reactivities at a plasma temperature 2.5 GK from different sources, obtained with different codes and different types of optical α+nucleus potentials. Also shown are the final ^{146}Sm/^{144}Sm production ratios $\mathcal{R}$ obtained for different ^{144}Sm(α,γ)^{148}Gd rates (and their reverse rates) in two models of the ccSN of a 25 $M_\odot$ star (ccSN-A [13, 31] and ccSN-B [2, 34]) and a SNIa model [33]. The values obtained with the optical potential of this work are given on the last line.

Type	Code	Reactivity	$\mathcal{R}$		
		(cm^3 s^{-1} mole^{-1})	ccSN-A	ccSN-B	SNIa
Equivalent Square Well [28]	CRSEC [1]	3.8×10^{-15}			
Folding (real), Woods-Saxon (imag.)	SMOKER[a] [29]	1.3×10^{-15}			
Woods-Saxon [20]	NON-SMOKER[a] [30]	1.9×10^{-15}	0.19	0.15	0.32
Woods-Saxon [20]	SMARAGD, this work	2.4×10^{-14}	0.11	0.06	
Energy-dep. Woods-Saxon [13]	MOST[a] [13], SMOKER[a] [29]	1.3×10^{-16}	0.44	0.39	
Energy-dep. Woods-Saxon [13]	SMARAGD, this work	2.2×10^{-15}	0.19	0.15	
Woods-Saxon [20], scaled α-width	SMARAGD, this work	1.2×10^{-14}	0.13	0.08	

[a] The codes SMOKER, NON-SMOKER, MOST used the same routine to calculate Coulomb barrier penetration.

(Rauscher 2013)

Table 3. Dependence of the $^{146}Sm/^{144}Sm$ ratio on various $^{148}Gd(\gamma,\alpha)$ rates for SNIa at different metallicities and (last line) for GCE calculations.

Z	RATH[a]	exp (α,γ) fit[b]	2013[c]
0.003	4.053×10^{-1}	7.408×10^{-1}	9.76×10^{-1}
0.006	3.705×10^{-1}	7.097×10^{-1}	8.90×10^{-1}
0.01	3.624×10^{-1}	6.850×10^{-1}	8.74×10^{-1}
0.012	3.762×10^{-1}	6.651×10^{-1}	9.05×10^{-1}
0.015	3.329×10^{-1}	6.319×10^{-1}	8.01×10^{-1}
0.02	3.161×10^{-1}	6.132×10^{-1}	7.62×10^{-1}
GCE τ=68 Myr	6.989×10^{-3}	1.050×10^{-2}	1.667×10^{-2}

[a]Rauscher & Thielemann (2000)

[b]Somorjai et al. (1998)

[c]Rauscher (2013)

Travaglio et al. 2014, ApJ in press

Radiogenic p-isotopes ^{92}Nb and ^{146}Sm in SNIa

	Meteorite	GCE
$^{146}Sm/^{144}Sm$	$(9.4 \pm 0.5)\times10^{-3}$	1.7×10^{-2}
Rausscher et al. (2013), new $^{148}Gd(\gamma,\alpha)^{144}Sm$ rate		

^{92}Nb

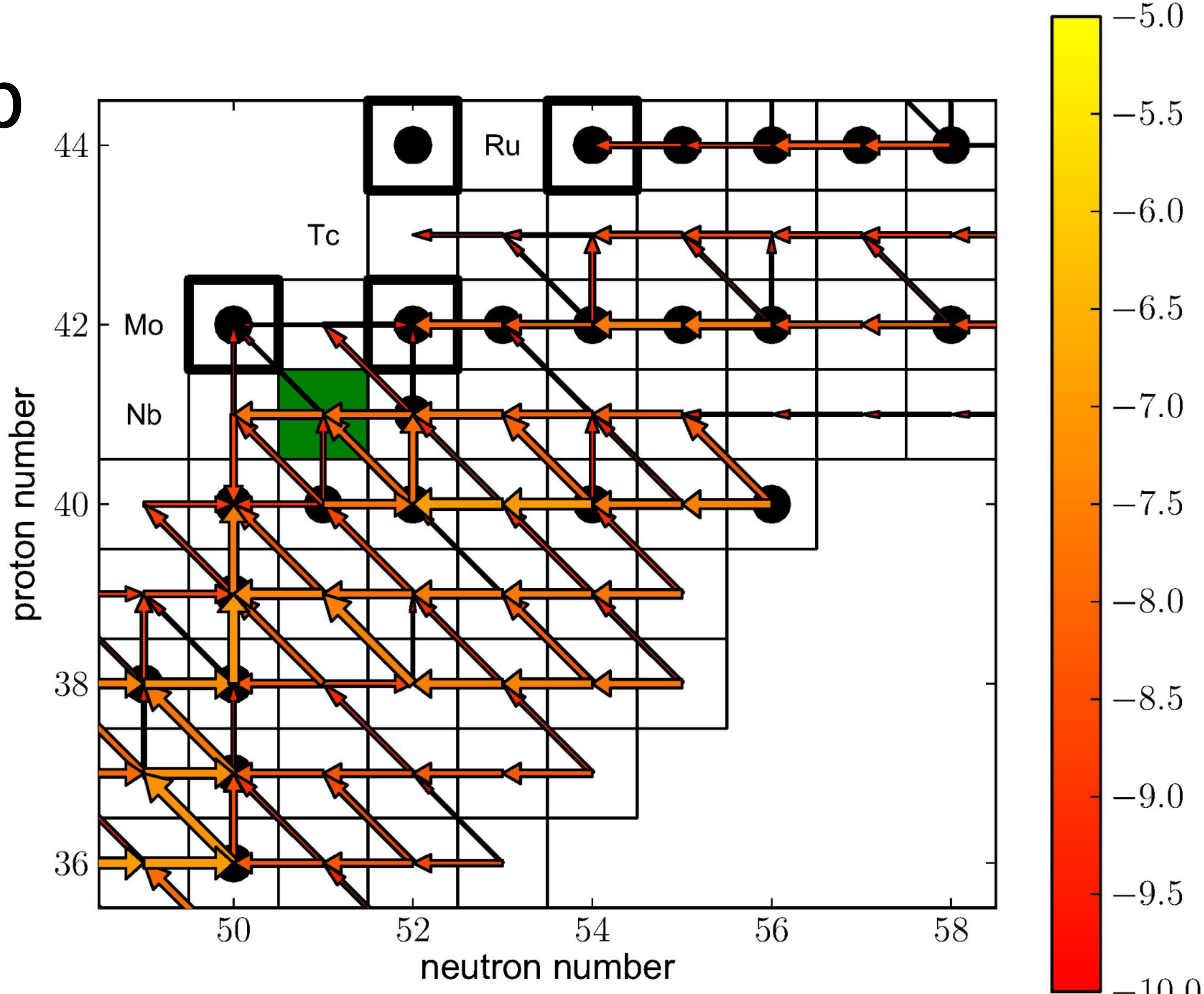
Ru
Tc
Mo
Nb
44
42
40
38
36
50
52
54
56
58
proton number
neutron number
−5.0
−5.5
−6.0
−6.5
−7.0
−7.5
−8.0
−8.5
−9.0
−9.5
−10.0
$\log_{10}(f)$

Table 4. Reactions affecting the ^{92}Nb/^{92}Mo ratio and their variation to explore the nuclear uncertainties; rate set MIN yields the minimal ratio, set MAX the maximal ratio. The arrows indicate whether a rate has been multiplied by a factor of two (arrow up) or divided by the same factor (arrow down). The modifications always apply to the rate and its reverse rate. In the last line there are the GCE calculations with these assumptions.

Reactions	Rate set MIN	Rate set MAX
^{91}Zr(p,γ)^{92}Nb	↓	↑
^{92}Zr(p,γ)^{93}Nb	↓	↑
^{92}Zr(p,n)^{92}Nb	↓	↑
^{91}Nb(n,γ)^{92}Nb	↑	↓
^{92}Nb(n,γ)^{93}Nb	↓	↑
^{91}Nb(p,γ)^{92}Mo	↑	↓
^{93}Nb(p,n)^{93}Mo	↑	↓
^{93}Mo(n,γ)^{94}Mo	↑	↓
GCE	1.660×10^{-5}	3.118×10^{-5}

Travaglio et al. 2014, ApJ in press

Radiogenic p-isotopes ^{92}Nb and ^{146}Sm in SNIa

	Meteorite	GCE
$^{92}Nb/^{92}Mo$	$(2.8 \pm 0.5)x10^{-5}$	$3.3x10^{-5}$

Uncertainties for $^{90}Zr(p, \gamma)^{91}Nb/2$, $^{91}Nb(n, \gamma)^{92}Nb x2$ $^{92}Nb(n,\gamma)^{93}Nb/2$

$^{146}Sm/^{144}Sm$	$(9.4 \pm 0.5)x10^{-3}$	$1.7x10^{-2}$

Rauscher et al. (2013), new $^{148}Gd(\gamma,\alpha)^{144}Sm$ rate

Travaglio et al. (2014, ApJ in press)